

Analysis the Process Ejection Cutting Soil of Chain Trenching Machine

Doan Diep, Hristo Beloev

Abstract: A chain trenching machine is a construction equipment used to dig trenches, especially for laying pipes or electrical cables, installing drainage, or in preparation for trench warfare. The analysis of the process working of chain trenching machine and its performance have been developed. The performance of chain trenching machine depends on various factors, one of these factors is process ejection cutting soil to a belt conveyer, which conveys the soil far enough to the side so it will not fall back into the trench.

When a chain trenching machine is digging a trench, its blades produce cuttings throughout their working sweep, and the working chain with cutting blades is mostly used as a inclined conveyer to remove the accumulated cutting soil and then eject the cutting soil on a conveyer. Process ejection spoil from cutting blade to the conveyer affects operational efficiency of chain trenching machine. If the cutting soil isn't ejected completely, part of the soil will remain on the working chain and return to the working surface, creating additional load and reducing the performance of the machine.

This paper deals with conditions to eject the spoil by the cutting blade to the conveyer. We study the relationship between drive sprocket rotational speed ω , forces and other factors to formulate the conditions to clear the spoil so as to avoid returning cutting soil to working surface. Analysis is used to determine the effect the various factors have upon performance rate and suggestions are made for chain trenching machine design that might further improve the process ejection.

Keywords: chain trenching machine, performance, process ejection, ejection of the spoil.

Chain trenching machine, cutting assembly and process ejection spoil

The chain trenching machine (fig.1) consists of a steel frame, usually mounted on crawlers 2, which is supported on the front end the power unit and at the rear end a steel framework holding the cutting assembly. This cutting assembly consists of a series of cutting blades carried on an endless chain. The cutting blades are drawn up the end of the trench either vertically or at an cutting angle Φ , cutting a thin slice of earth from bottom to top. At the end of their up ward movement the cutting blades empty their spoil on the endless belt 4, which conveys the spoil far enough to the side so it will not fall back into the trench.

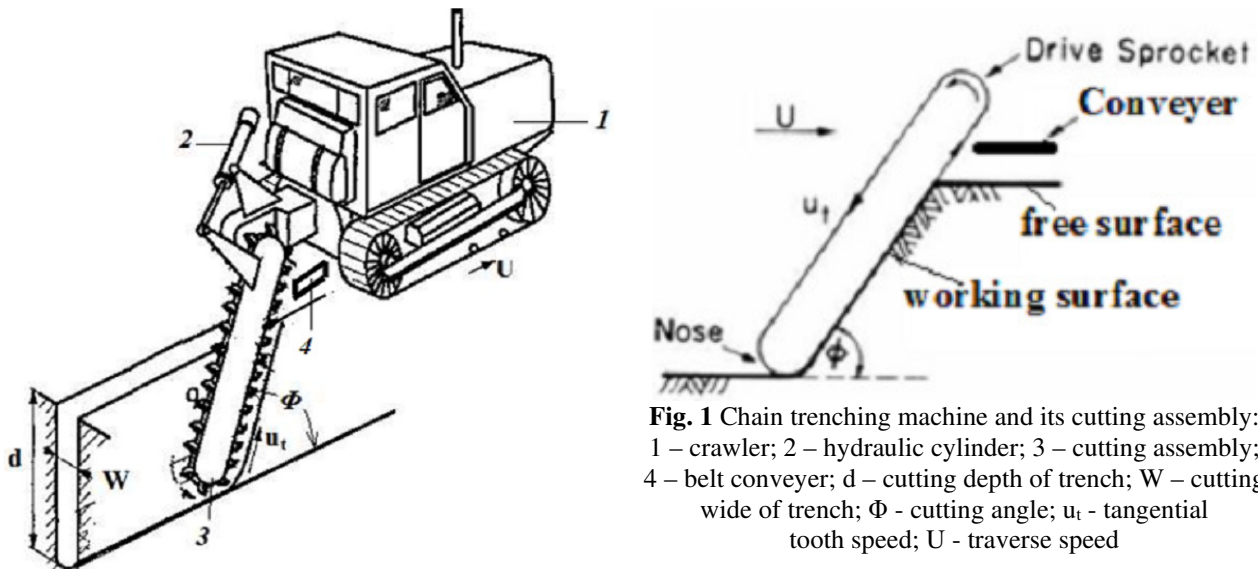


Fig. 1 Chain trenching machine and its cutting assembly:
1 – crawler; 2 – hydraulic cylinder; 3 – cutting assembly;
4 – belt conveyer; d – cutting depth of trench; W – cutting
wide of trench; Φ - cutting angle; u_t - tangential
tooth speed; U - traverse speed

The cutting assembly usually consists of a maneuverable steel frame that carries the endless working chain. The endless working chain which carries cutting blades to cut the soil from working surface. The cutting blades on endless chain are laid out in a repeating pattern so that is symmetrical about the center line of the chain face. The free end of cutting assembly is known as the nose. The nose is usually the trailing end of the cutting assembly. The sprocket at the nose, which normally is not driven, is the nose sprocket.

When chain trenching machine is trenching, it is normally operated with the drive sprocket clear of the work and is rotating so as to pull the active side of the working chain towards itself in tension. The chain with cutting blades tends to cut and convey cuttings to the free surface, and process ejection of the spoil begins when the cutting blade begins rotating with the drive sprocket (at point O fig. 2). When the spoil rotates with the drive sprocket, on its acting forces such as centrifugal force, Coriolis force, gravity force, Friction force, reaction force (fig. 2) and sum of these five vector forces creates acceleration to slide the spoil along the leading face of the cutting blade until the point O₁. From point O₁ the spoil begins projectile motion and drops on the belt conveyer (fig. 2).

Simulation model of ejection process

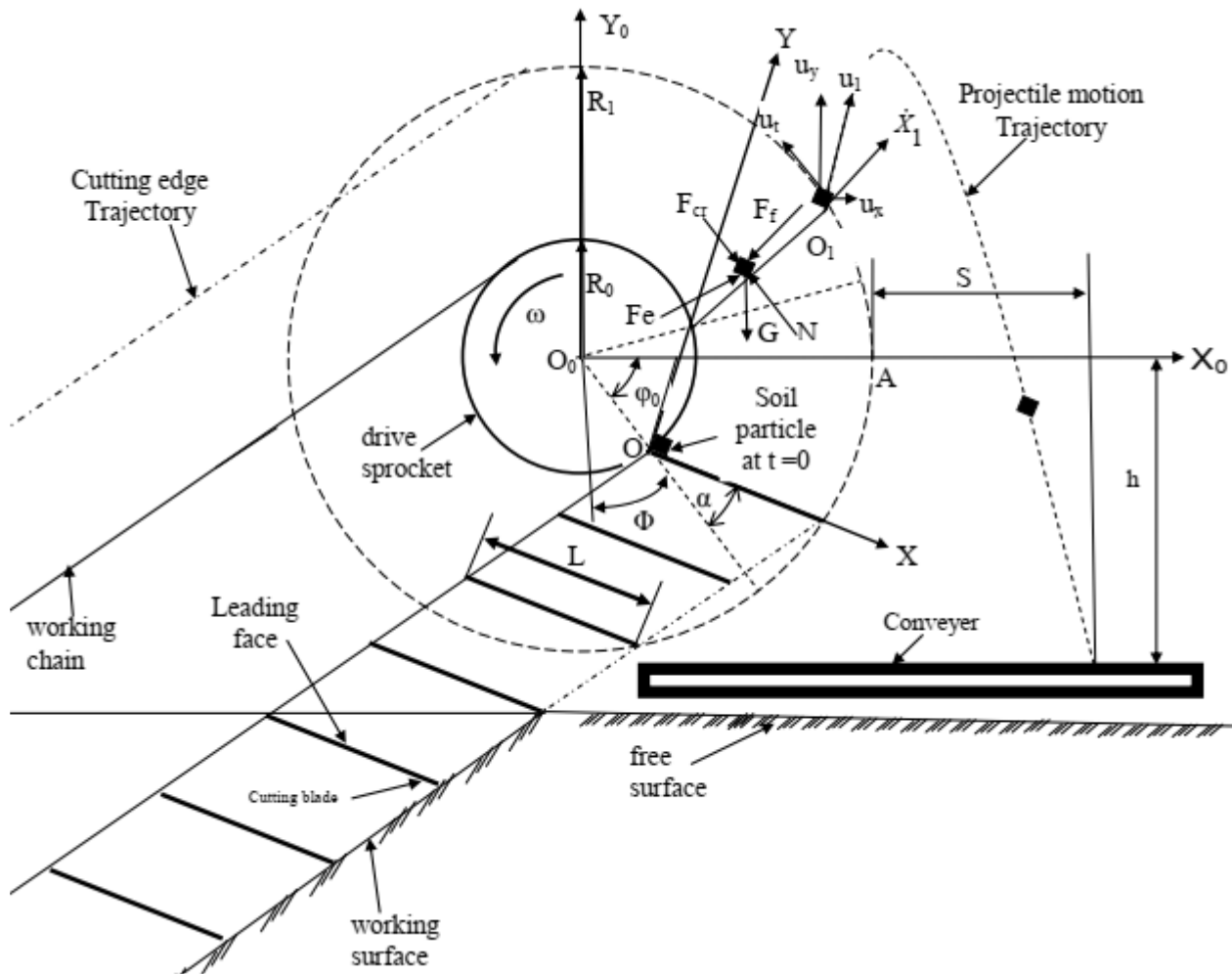


Fig. 2 Simulation model of ejection process: ω - drive sprocket angular speed; R_0 - drive sprocket radius; R_1 - outer radius of cutting edge trajectory; S –horizontal projectile distance relative to the closest point A of cutting edge trajectory; α - rake angle, Φ – cutting angle, L – length of leading face

In order to establish a simulation model of ejection process, we offer 2 coordinate systems, which are described in the Figure 2 as follow:

- The $X_0O_0Y_0$ coordinate system is attached to the body of the machine, O_0X_0 and O_0Y_0 directions are defined from origin O_0 in the centre of drive sprocket, with the X_0Y_0 plane in the plane of the bar and the O_0X_0 direction parallel to the traverse direction of the machine.

- The XOY coordinate system, with OX and OY directions are defined from origin O . Origin O is located at the joint point of the cutting blade and OX axis is laid on the front cutting blade face.

Therefore, the XOY coordinate system is rotated with drive sprocket angular speed ω in relation to the $X_0O_0Y_0$ coordinate system.

The forces acting on the soil particles

- Centrifugal force \vec{F}_e

$$\vec{F}_e = m.\omega^2.\vec{R} = m.\omega^2.\left[(R_0.\cos\alpha + X).\vec{i} - R_0.\sin\alpha.\vec{j}\right] \quad (1)$$

Where: \vec{i} , \vec{j} are the unit vectors of OX and OY axes, m is mass of a soil particle

- Coriolis force

$$\vec{F}_{cr} = 2.m.\vec{\omega} \times \vec{u}_r$$

Where: \vec{u}_r is sliding velocity vector of the soil particle, relatively to coordinate system $X_0O_0Y_0$.

$$\vec{u}_r = \dot{X}.\vec{i}$$

$$\vec{\omega} = \omega.\vec{k}$$

$$\vec{k} \text{ is a unit vector of OZ axis; } \vec{k} = \vec{i} \times \vec{j}; \vec{i} = \vec{j} \times \vec{k}; \vec{j} = \vec{k} \times \vec{i}$$

Therefore:

$$\vec{F}_{cr} = 2.m.\vec{\omega} \times \vec{u}_r = 2m.\dot{X}.\omega.\vec{k} \times \vec{i} = -2m.\dot{X}.\omega.\vec{j} \quad (2)$$

- Gravitational force

$$\vec{G} = -mg.\sin(\varphi + \alpha).\vec{i} - mg.\cos(\varphi + \alpha).\vec{j} \quad (3)$$

- Friction force

$$\vec{F}_f = -(f.N + C).\vec{i} \quad (4)$$

Where: C is soil cohesion

- Reaction force of cutting blade:

$$\vec{N} = N.\vec{j} \quad (5)$$

The equation sliding motion of soil particle along leading surface:

Substitute the (1), (2), (3), (4), (5) to form vector equation of sliding motion of soil particle:

$$m.\ddot{X}.\vec{i} = m.\omega^2.\left[(R_0.\cos\alpha + X).\vec{i} - R_0.\sin\alpha.\vec{j}\right] - 2m.\dot{X}.\omega.\vec{j} - mg.\sin(\varphi + \alpha).\vec{i} - mg.\cos(\varphi + \alpha).\vec{j} - (f.N + C).\vec{i} + N.\vec{j}$$

In terms of axes OX, OY we have the algebraic equation:

$$-m.\omega^2.R_0.\sin\alpha.\vec{j} - 2m.\dot{X}.\omega.\vec{j} - mg.\cos(\varphi + \alpha).\vec{j} + N.\vec{j} = 0 \quad (6)$$

$$N = m.\omega^2.R_0.\sin\alpha + 2m.\dot{X}.\omega + mg.\cos(\varphi + \alpha) \quad (7)$$

Substitute equation(7) into the equation (6), we have:

$$m.\ddot{X} = m.\omega^2.(R_0.\cos\alpha + X) - mg.\sin(\varphi + \alpha) - \left[f.\left(m.\omega^2.R_0.\sin\alpha + 2m.\dot{X}.\omega + mg.\cos(\varphi + \alpha) \right) + C \right]$$

$$\ddot{X} = \omega^2.(R_0.\cos\alpha + X) - g.\sin(\varphi + \alpha) - \left[f.\left(\omega^2.R_0.\sin\alpha + 2.\dot{X}.\omega + g.\cos(\varphi + \alpha) \right) + C/m \right] \quad (9)$$

Where: φ - angular displacement is defined as:

$$\varphi = \varphi_0 + \omega.t = \phi - 90^0 + \omega.t$$

Equation (9) is the second order differential equation and we can solve it by numerical method with following informations:

1. Starting moment of sliding motion: $X(t = 0) = 0; \dot{X}(t = 0) = 0;$
2. Ending moment of sliding motion: $X(t) = L = X_1$

Where L is the long of the rake face of cutting blade (fig. 2).

3. Ending of sliding velocity at point O_1 - \dot{X}_1 , m/s

Velocities of soil particle in relation to coordinate system $X_0O_0Y_0$

Designating: \vec{u} is absolute vector velocity \vec{u} of soil particle in relation to $X_0O_0Y_0$; \vec{u}_r is sliding vector velocity of the soil particle in relation to $X_0O_0Y_0$; \vec{u}_t is tangential vector velocity of the soil particle in relation to $X_0O_0Y_0$.

Absolute vector velocity \vec{u} of soil particle in relation to $X_0O_0Y_0$ is defined as:

$$\vec{u} = \vec{u}_r + \vec{u}_t \quad (10)$$

- Sliding vector velocity \vec{u}_r of the soil particle in relation to $X_0O_0Y_0$ defined as:

$$\vec{u}_r = \dot{X} \cdot \cos(\varphi + \alpha) \cdot \vec{i}_0 + \dot{X} \cdot \sin(\varphi + \alpha) \cdot \vec{j}_0 \quad (11)$$

Where: \vec{i}_0, \vec{j}_0 are the unit vectors of OX_0 and OY_0 axes.

- Tangential vector velocity of the soil particle in relation to $X_0O_0Y_0$ is defined as:

$$\vec{u}_t = \vec{\omega} \times \vec{R} \quad (12)$$

Radius vector \vec{R} in relation to $X_0O_0Y_0$ is defined as:

$$\begin{aligned} \vec{R} &= \vec{O}_0O + \vec{X} = R_0 \cos \varphi \cdot \vec{i}_0 + R_0 \sin \varphi \cdot \vec{j}_0 + X \cdot \cos(\alpha + \varphi) \cdot \vec{i}_0 + X \sin(\alpha + \varphi) \cdot \vec{j}_0 = \\ &= [R_0 \cos \varphi + X \cdot \cos(\alpha + \varphi)] \cdot \vec{i}_0 + [R_0 \sin \varphi + X \sin(\alpha + \varphi)] \cdot \vec{j}_0 \end{aligned} \quad (13)$$

Substitute equation (13) into the equation (12) we have:

$$\begin{aligned} \vec{u}_t &= \vec{\omega} \times \vec{R} = \omega \vec{k}_0 \times \left\{ [R_0 \cos \varphi + X \cdot \cos(\alpha + \varphi)] \cdot \vec{i}_0 + [R_0 \sin \varphi + X \sin(\alpha + \varphi)] \cdot \vec{j}_0 \right\} = \\ &= -\omega \cdot [R_0 \sin \varphi + X \sin(\alpha + \varphi)] \cdot \vec{i}_0 + \omega \cdot [R_0 \cos \varphi + X \cdot \cos(\alpha + \varphi)] \cdot \vec{j}_0 \end{aligned} \quad (14)$$

Substitute equations (14) and (11) into the equation (10) we have absolute vector velocity \vec{u} of soil particle relatively to $X_0O_0Y_0$ is defined as:

$$\begin{aligned} \vec{u} &= \dot{X} \cdot \cos(\varphi + \alpha) \cdot \vec{i}_0 + \dot{X} \cdot \sin(\varphi + \alpha) \cdot \vec{j}_0 - \omega [R_0 \sin \varphi + X \sin(\alpha + \varphi)] \cdot \vec{i}_0 + \omega [R_0 \cos \varphi + X \cdot \cos(\alpha + \varphi)] \cdot \vec{j}_0; \\ \vec{u} &= \left\{ \dot{X} \cdot \cos(\varphi + \alpha) - \omega [R_0 \sin \varphi + X \cdot \sin(\alpha + \varphi)] \right\} \cdot \vec{i}_0 + \left\{ \dot{X} \cdot \sin(\varphi + \alpha) + \omega [R_0 \cos \varphi + X \cdot \cos(\alpha + \varphi)] \right\} \cdot \vec{j}_0 \end{aligned} \quad (15)$$

Projectile motion of soil particle in relation to $X_0O_0Y_0$

In the figure 2, at point O_1 the process sliding is finished and projectile motion is beginning. The coordinates of soil particle at point O_1 in relation to $X_0O_0Y_0$ is defined as:

$$X_1 = R_0 \cos \varphi + L \cdot \cos(\varphi + \alpha); Y_1 = R_0 \sin \varphi + L \sin(\varphi + \alpha) \quad (16)$$

Designating u_1 is the initial projectile velocity of soil particle at point O_1 – u_1 can be resolved to initial horizontal component u_x and initial vertical component u_y and they're is defined as:

$$u_x = \dot{X}_1 \cdot \cos(\varphi + \alpha) - \omega \cdot [R_0 \sin \varphi + X \cdot \sin(\alpha + \varphi)], \quad (17)$$

$$u_y = \dot{X}_1 \cdot \sin(\varphi + \alpha) + \omega \cdot [R_0 \cos \varphi + X \cdot \cos(\alpha + \varphi)]. \quad (18)$$

Displacement coordinates of soil particle in projectile motion are defined as:

$$X = X_1 + u_x \cdot t_1 \quad (19)$$

$$Y = Y_1 + u_y \cdot t_1 - \frac{gt^2}{2} \quad (20)$$

Where t_1 is time of projectile motion.

Designating t_e is total time of projectile motion, the coordinates of soil particle in the end of projectile motion are defined as:

$$X = X_1 + u_x \cdot t_e \quad (21)$$

$$Y_e = Y_1 + u_y t_1 - \frac{gt_e^2}{2} = -h \tag{22}$$

Total time of projectile motion t_e is defined as:

$$t_e = \frac{u_y + \sqrt{u_y^2 + 2.g.(Y_1 + h)}}{g} \tag{23}$$

Horizontal projectile distance relative to the closest point of cutting edge trajectory A is defined as:

$$S = X_1 + u_x \cdot \frac{u_y + \sqrt{u_y^2 + 2.g.(Y_1 + h)}}{g} - R_1 \tag{24}$$

The illustrations of the solve numerical method results

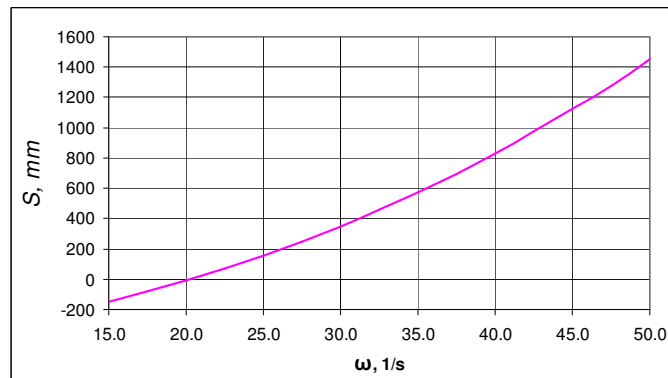


Fig. 3 Plotted against ω

(For the given parameters: $R_0 = 0.2$ m; $L = 0.05$ m; $\alpha = 450$; $\phi = 400$, $h = 0,25$ m)

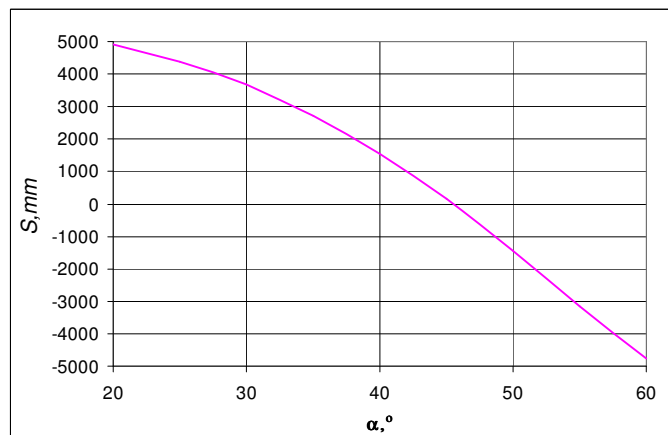


Fig. 4 S plotted against α

(For the given parameters: $R_0 = 0.2$; $L = 0.05$ m; $\omega = 25$ rad/s; $\phi = 40^\circ$, $h = 0,25$ m)

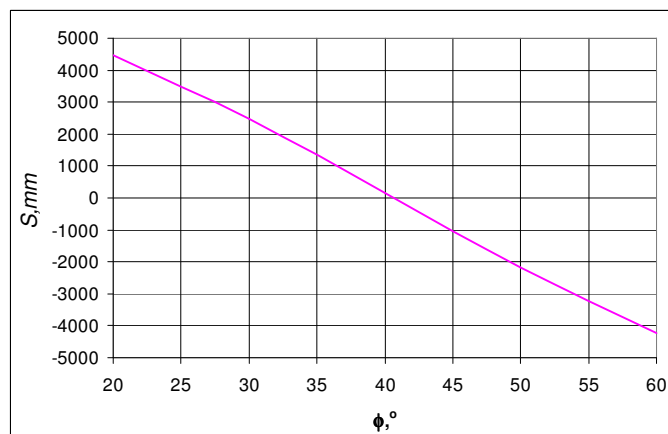


Fig. 5 S plotted against Φ

(For the given parameters: $R_0 = 0.2$ m; $L = 0.05$ m; $\alpha = 45^\circ$; $\omega = 25$ rad/s, $h = 0,25$ m)

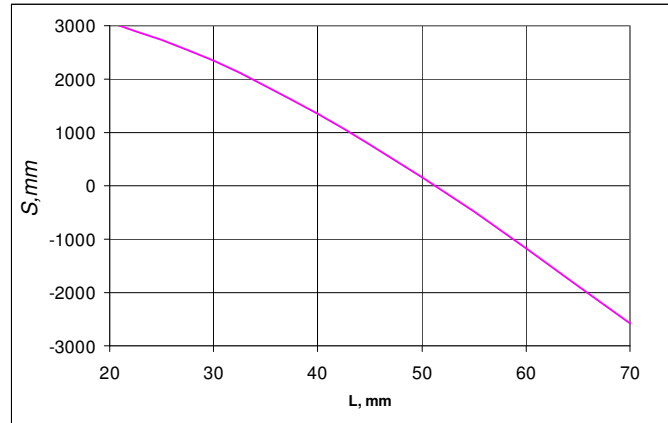


Fig. 6 S plotted against the leng of leading face L

(For the given parameters: $R_0 = 0.2$; $\alpha = 45^\circ$; $\omega = 25^\circ$; $\phi = 40^\circ$; $h = 0,25$ m)

DISCUSSIONS AND CONCLUSIONS

- Figure 3 show the displacement of soil particle increase with the rotational speed ω . For the given parameters: $R_0 = 0.2$ m; $L = 0.05$ m; $\alpha = 45^\circ$; $\phi = 40^\circ$, $h = 0,25$ m. If $\omega < 20$ 1/s, process ejection is not completed, part of the spoil remain on the working chain and return to the working surface.

- Meanwhile, the figure 4 illustrates the displacement of soil particle decreases when the rake angle α increases, because of incline of leading face and create difficulties for ejection. For the given parameters: $R_0 = 0.2$; $L = 0.05$ m; $\omega = 25$ 1/s; $\phi = 40^\circ$ $h = 0,25$ m, if α rake angle $> 46^\circ$, process ejection is not completed, part of the spoil remain on the working chain and return to the working surface.

- The displacement of soil particle decreases when the cutting angle Φ increases, because of coinciding inclining the cutting angle and inclining of the leading face and create difficulties for ejection. For the given parameters: $R_0 = 0.2$ m; $L = 0.05$ m; $\alpha = 45^\circ$; $\omega = 25$ 1/s, $h = 0,25$ m. If cutting angle $\Phi > 41^\circ$, process ejection is not completed, part of the spoil remain on the working chain and return to the working surface.

- Figure 7 illustrates that, the length of leading face L increases, displacement of soil particle decreases, because sliding process along leading face is longer. With some parameters: $R_0 = 0.2$ m; $\alpha = 45^\circ$; $\omega = 25^\circ$; $\phi = 40^\circ$; $h = 0,25$ m, if $L > 52$ mm, the part of the spoil remain on the cutting blade.

Results of this analysis give us suggestions in design and choosing working parameters of endless chain trenching machine that might further improve the process ejection of cutting soil.

REFERENCES

- [1] Arkady N. Schipunov (2013) The premiseses of the improvement screw cleaneres of a soil for removing the frozen working soil of the zone executive organ unbucket chain trencheres
- [2] Barry A. (1989) Factors affecting rates of ice cutting with a chain saw. USA Cold Regions Research and Engineering Laboratory, Special Report.
- [3] Basov I., Slepchenko V., (1998) Substantiation of selection of the excavator blade width trench beskovshovosh, Interstroyneh-98: Proceedings of the Intern. nauch.-techn. Conf. Voronezh Voronezh State. ar-hit. -BUD. Academy, pp 97- 98.
- [4] Beloev, H., Dimitrov, P., Kangalov, P., Stoyanov, K., Ilieva D. (2012) Machine operation tests on anti-erosion machine-tractor aggregates for composting and vertical mulching. *Mendeltech international 2012*. International scientific conference, Brno,.
- [5] Giezen, M. (1993). Rock properties relevant to tool wear and production of rock cutting trenchers, Memoirs of the Centre of Engineering Geology, Mining and Petroleum Engineering, 110, TU Delft, Delft, The Netherlands.
- [6] Homelite. (1979) 550 Professional chain saw operation and maintenance manual, 1st Edition, Part No. 17134-A. Charlotte, North Carolina: Homelite Division of Textron Inc.

- [7] Ian W. Farmer Associates Ltd. Performance of chain trenchers in mixed ground. . Journal of Construction Engineering and Management, 1996, pp. 115-118.
- [8] Mellor, M. (1976) Mechanics of cutting and boring, part III: Kinematics of continuous belt machines. USA Cold Regions Research and Engineering Laboratory, CRREL Report 76-79.
- [9] Sweeney M., Leng S.A., Pettifer G.S. &Haustermans L. (2005) Performance of chain trenchers in rock: a database and a preliminary predictive model. In: Sweeney M. (ed.) Proc. Conf. on Terrain and Geohazard Challenges Facing Onshore Oil and Gas Pipelines, Thomas Telford, London.
- [10] Sweeney M., Pettifer G.S., Shilston D.T., Bel-Ford P. & Stockbridge M. (2005) In Salah Gas Project, Algeria – Part 3: Prediction and performance of large chain trenchers on a desert pipeline project. In: Sweeney M. (ed.) Proc. Conf. on Terrain and Geohazard Challenges Facing Onshore Oil and Gas Pipelines, Thomas Telford, London.
- [11] Utinov A.B. (2007) Studying technical parameters of the soil scraper with the aim for improving performance of unbuckled chain trencher.
- [12] Vahrushev A.A., R.N. Kotik. (2014) Analysis of the process of the displacement destroyed frozen soil. international conference of students and young scientists. Russia, Tomsk, pp. 728 - 731
- [13] Vartanov S. H. (1983) Improving the technical level of chain trenching machines // Mechanization stroitelstva, number 2, pp 6-8.

CONTACTS

Doan Dinh Diep, Department of Construction machines, Hanoi University of Architecture, Vietnam, E-mail: doandiep2364@gmail.com

Hristo Beloev, Department of Agricultural Machinery, Agrarian and Industrial Faculty, University of Ruse “Angel Kanchev”, 8 Studentska str., 7017 Ruse, Bulgaria, e-mail: hbeloev@uni-ruse.bg